P8.18 BAYESIAN RETRIEVAL OF COMPLETE POSTERIOR PDFS OF OCEANIC RAIN RATE FROM MICROWAVE OBSERVATIONS

J.-Y. Christine Chiu*
JCET/UMBC, Baltimore, Maryland
Grant W. Petty
University of Wisconsin-Madison, Madison, Wisconsin

1. INTRODUCTION

To provide a long-term global basis of precipitation information, satellite passive microwave observations have been widely used in the past decades to estimate surface rain rate. Among various approaches, some algorithms have invoked Bayes theorem to retrieve a single instantaneous rain rate and vertical hydrometeor profiles (Evans et al., 1995; Olson et al., 1996; Kummerow et al., 1996; Bauer et al., 2001). Bayes theorem offers a rigorous theoretical framework for retrieval algorithms, however, up to now, we are unaware of any algorithm that fully exploits Bayes theorem to provide a continuous posterior probability distribution function (PDF) of rain rate.

We present a new Bayesian algorithm for rain rate retrieval over the ocean in this paper. A unique property of this new algorithm is that the result of the algorithm is not a single "best" rain rate but rather a complete posterior PDF, which is potentially beneficial to data assimilation applications. The other key element of the algorithm is the characterization of relationship between microwave radiance and surface rain rate, which depends on both the physical and statistical properties of rainfall, as well as the beam-filling effects. Since actual match-up data from microwave and rainfall measurements or detailed model simulations do not exist in a sufficient quantity, we rely on simulated data derived from high-resolution radar composites, and explicit functional models to facilitate our algorithm.

* *Corresponding author address:* J.-Y. Christine Chiu,1000 Hilltop Circle, Baltimore, MD 21250; e-mail: cchiu@climate.gsfc.nasa.gov.

2. BASIS OF ALGORITHM

This new Bayesian algorithm retrieves surface rain rate primarily from the Tropical Rainfall Measuring Mission (TRMM) Microwave Imager (TMI) measurements. Due to the ambiguity of rain rate retrieval from microwave radiance, we used the attenuation index *P* (Petty, 1994) to construct our algorithm. The attenuation indices at the TMI channels of 10.65, 19.35, and 37.00 GHz are hereafter denoted as P_{10}, P_{19}, and P_{37}, respectively.

2.1 *Theoretical Framework*

Bayes theorem states that given the data **P** (e.g., microwave observations), the distribution of the parameters **R** (e.g., rain rate) is proportional to the conditional likelihood times the prior distribution:

$$\pi(R \mid P) = \frac{f(P \mid R) \cdot \pi(R)}{\int f(P \mid R) \cdot \pi(R) \cdot dR}. \qquad (1)$$

f(P|R) is a conditional probability density function that expresses statistical and physical information about the relationship between **P** and R. π(R) describes our prior knowledge of rain rate. The interactions of the physical and statistic conditional and the prior probability distribution determines the so-called *posterior distribution*, π(R|**P**), the new PDF of rain rate R in light of the observations **P**. Normally, the effect of **P** is to reduce the spread of π(R|**P**) relative to π(R); and the degree of reduction is a measure of the information content of **P.**

In this study, the distribution of **P** at a given rain rate is approached successively:

$$\begin{aligned} f(P \mid R) &= f(P_{10}, P_{19}, P_{37} \mid R) \\ &= f(P_{37} \mid R) f(P_{19} \mid P_{37}, R) f(P_{10} \mid P_{19}, P_{37}, R). \end{aligned} \qquad (2)$$

Each conditional PDF was modeled by explicit functions. For example, the conditional PDF of P_{37} at a given rain rate was characterized by

$$f(P_{37} \mid R) \propto P_{37}(a - P_{37}) \exp\left[-\frac{1}{2\sigma_3^2}(P_{37} - \mu_3)^2\right], \quad (3)$$

where *a* is a constant and P_{37} is in the range between 0 and *a*. μ_3 and σ_3 are functions of rain rate and determined by fitting to the data. In addition, the prior distribution of rain rate is parameterized by a lognormal function. Once the conditional and prior likelihoods are specified, the complete posterior PDF can be computed by equation (1).

2.2 *Radar-Radiative Simulations*

The specifications of those parameters in equation (2) and (3) rely on the training datasets that provide sufficient and appropriate physical and statistical dependency of microwave signal on precipitation rate. In an attempt to account for the inhomogeneity of rain clouds, we used high-resolution NWS WSR-88D composite reflectivity data to include realistically spatial precipitation structures. These reflectivity data have an hourly temporal resolution and a spatial resolution of 1km. Surface rain rate for each radar pixel was modeled by the Marshall-Palmer Z-R equation. The simulated rain cloud field was then applied into a simplified plane-parallel radiative transfer model to compute the attenuation index field.

To ensure the representativeness of the radar-radiative simulations, figure 1 depicts the comparisons of the multichannel relationships between the model-simulated and TMI-observed attenuation index fields. Surprisingly, the 3-D structure of the attenuation index from radar simulations demonstrates a great similarity to the actual TMI observations in both locations and orientation of the 2-D slices. Theoretically, in a homogeneous case of rain cloud, a unique non-linear relationship in **P** is expected. However, in reality, due to various beam-fillings effects, **P** scatters in 3-D space and its distribution forms a cloud on the 2-D contours, as shown in both observations and simulations.

3. Results

3.1 *Complete Posterior PDF*

Figure 2 demonstrates examples of the derived posterior PDFs of rain rate at given microwave attenuation index vectors. These posterior distributions of rain rate have a single maximum over the entire range, showing how the algorithm modifies the prior rain rate distribution after microwave data are seen. Based on these continuous probability distributions, the statistical properties of retrieved rain rates, such as the mean and deviation, can be easily defined.

3.2 *Comparisons with PR and GPROF*

We used four verification measures to quantify statistical differences between the retrieved rain rate and the measurements from TRMM Precipitation Radar (PR). The validation measurements include the bias, the root-mean-square error, and the correlation coefficient, and the Heidke Skill Score (HSS). We also compared our retrieval with that of the Goddard Profiling algorithm (GPROF). Since PR and GPORF provide single-pixel rain rates only, we used two common estimates to represent the "best" retrieved rain rate: the mean value (MEAN), and the maximum likelihood estimate (MLE). These two estimates are hereafter denoted as the Bayesian-MEAN and the Bayesian-MLE, respectively.

Since validation metrics are highly context sensitive, depending on the characteristics of the validation dataset as well as the performance of the algorithm, validation statistics cannot easily be interpreted in isolation but rather should be used as a basis for comparing different algorithms applied to the identical validation dataset. Therefore, we selected several TMI-PR match-up datasets for various precipitation systems for the validation. Those datasets include a typhoon case with TMI orbit number 336, twelve cases over the ocean from Bauer et al. (2001), 88 heavy and widespread rain events in 1998, and randomly-selected 118 orbit files in April 1998.

Table 1 summarizes the calculated bias, the root-mean-squared error, and the correlation coefficient for each validation dataset. The performance of our Bayesian algorithm is found to be comparable to that of the GPROF, while our algorithm has an added advantage of posterior rain rate PDFs.

In order to obtain a direct sense of how different the retrieval from each algorithm behaves, PR interpolated and algorithm-retrieved rain rate are mapped for the typhoon case (figure 3). Qualitatively, rain maps exhibit that these two algorithms are able to retrieve the eye, two separate rain bands, and the overall cyclonic structure of the typhoon. Quantitatively, the retrieval from the new algorithm has a similar magnitude of rain rates to the PR data and GPROF retrievals. However, the Bayesian-MLE retrieved rain rates demonstrate noticeable underestimations of rainfall rate, and thus show a negative bias in table 1.

4. Conclusions

This paper has presented a new Bayesian rain rate retrieval algorithm and applied this algorithm to real TMI data over the ocean. Validations against PR rain rates have indicated that the performance of our new algorithm is comparable to the Goddard Profiling algorithm in terms of commonly used verification metrics, while our new algorithm has an additional advantage of providing a complete continuous posterior probability distribution of surface rain rate.

References

Bauer, P., P. Amayenc, C. D. Kummerow and E. A. Smith, 2001: Over-ocean rain fall retrieval from multisensor data of the Tropical Rainfall Measuring Mission. Part II: Algorithm implementation. *J. Atmos. Oceanic Technol.*, **18**, 1838-1855.

Evans, K. F., J. Turk, T. Wong and G. L. Stephens, 1995: Bayesian approach to microwave precipitation profile retrieval. *J. Appl. Meteor.*, **34**, 260-279.

Kummerow, C., W. S. Olson and L. Giglio, 1996: A simplified scheme for obtaining precipitation and vertical hydrometeor profiles from passive microwave sensors. *IEEE Trans. Geosci. Remote Sens.*, **34**, 1213-1232.

Olson, W. S., C. D. Kummerow, G. M. Heymsfield and L. Giglio, 1996: A method for combined passive-active microwave retrievals of cloud and precipitation profiles. *J. Appl. Meteor.*, **35**, 1763-1789.

Petty, G. W., 1994: Physical retrievals of over-ocean rain rate from multichannel microwave imagery. Part II: Algorithm implementation. *Meteorol. Atmos. Phys.*, **54**, 101-121.

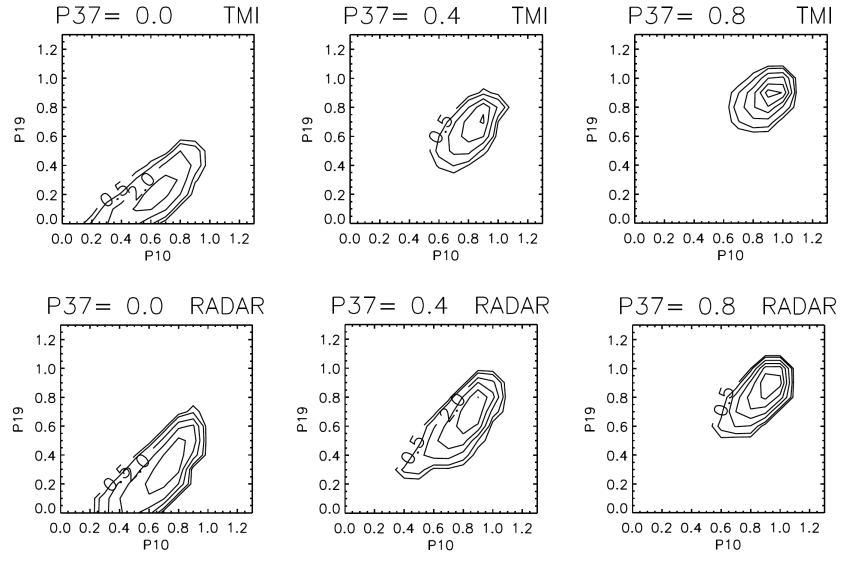

Figure 1. Contours of the number of pixels based on TMI data (the first row) and radar-radiative simulations (the second row). Contours are logarithmically spaced; actual value is 10^x where x is the contour label. x is plotted for values of [0.5, 1, 2, 3, 4, 5].

Table 1. Summary of the bias, root-mean-squared error (rms), and the correlation coefficient for GPROF and the Bayesian algorithm against each validation dataset. The unit of the bias and rms is mm/hr.

	Orbit 336			Bauer's case			Heavy widespread			Apr. 1998 random		
Algorithm	Bias	RMS	Corr	Bias	RMS	Corr	Bias	RMS	Corr	Bias	RMS	Corr
GPROF	-0.22	2.68	0.88	-0.22	1.64	0.76	-0.15	4.08	0.75	-0.21	1.18	0.78
BAYE.-MEAN	0.00	2.89	0.85	0.08	1.84	0.71	1.30	5.03	0.68	0.03	1.26	0.78
BAYE.-MLE	-1.04	3.75	0.85	-0.29	1.80	0.74	-0.19	4.49	0.69	-0.01	1.21	0.75

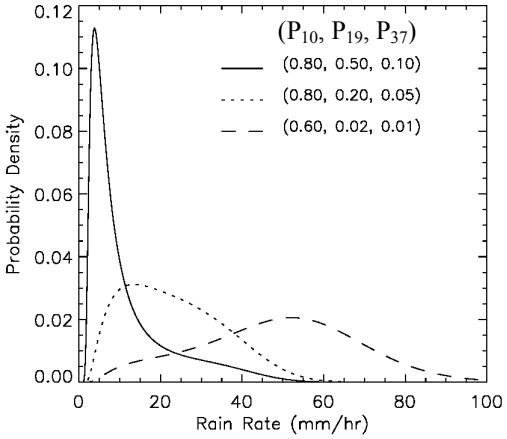

Figure 2. Examples of derived posterior rain rate distributions at some given **P**. The three numbers in parentheses represent the observation vector **P** = (P_{10}, P_{19}, P_{37}).

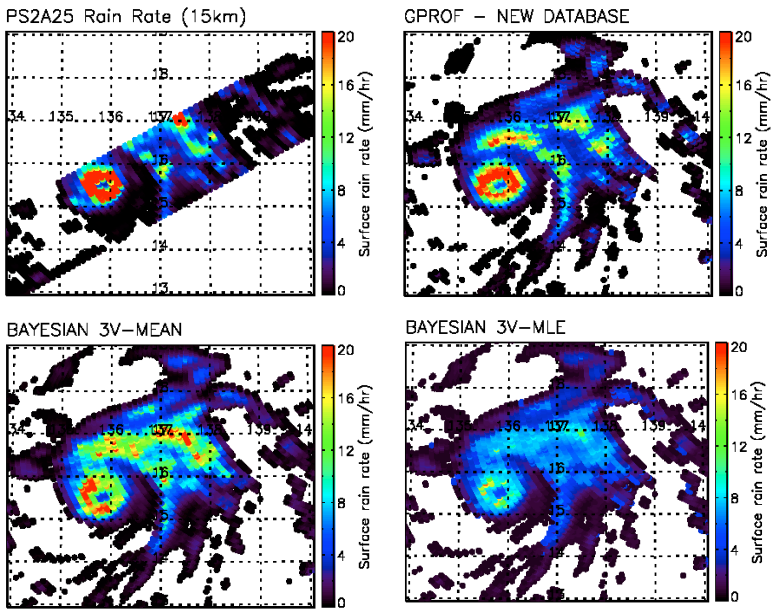

Figure 3. Maps of PR interpolated rain rate with 15-km resolution, and retrieved surface rain rate from GPROF, Bayesian-MEAN, and Bayesian-MLE for TRMM/TMI orbit 336.